Earth Syst. Sci. Data Discuss., 5, 853–891, 2012
www.earth-syst-sci-data-discuss.net/5/853/2012/
doi:10.5194/essdd-5-853-2012

Open Access Earth System Science Data Discussions

Calibration procedures and first data set of Southern Ocean chlorophyll *a* profiles collected by elephant seal equipped with a newly developed CTD-fluorescence tags

C. Guinet[1], X. Xing[2,3], E. Walker[4], P. Monestiez[4], S. Marchand[5], B. Picard[1], T. Jaud[1], M. Authier[1], C.'Cotté[1,6], A. C. Dragon[1], E. Diamond[2], D. Antoine[2], P. Lovell[7], S. Blain[8], F. D'Ortenzio[2], and H. Claustre[2]

[1]Centre d'Etudes Biologiques de Chizé-CNRS, Villiers en Bois, France
[2]Laboratoire d'Océanographie de Villefranche, Villefranche-sur-Mer, France
[3]Ocean University of China, Qingdao, China
[4]Unité Biostatistique et Processus Spatiaux-INRA, Avignon, France
[5]Muséum national d'histoire naturelle, DMPA USM 402/LOCEAN, Paris, France
[6]Université Paris VI, DMPA USM402/LOCEAN, Paris, France
[7]Sea Mammal Research Unit, University of St. Andrews, St. Andrews, Scotland
[8]Laboratoire d'Océanographie Microbienne, Université Paris VI, Banyuls sur mer, France

Received: 21 June 2012 – Accepted: 19 July 2012 – Published: 23 August 2012

Correspondence to: C. Guinet (guinet@cebc.cnrs.fr)

Published by Copernicus Publications.

ESSDD

5, 853–891, 2012

Abstract

In-situ observation of the marine environment has traditionally relied on ship-based platforms. The obvious consequence is that physical and biogeochemical properties have been dramatically undersampled, especially in the remote Southern Ocean (SO). The difficulty in obtaining in situ data represents the major limitations to our understanding, and interpretation of the coupling between physical forcing and the biogeochemical response. Southern elephant seals (*Mirounga leonina*) equipped with a new generation of oceanographic sensors can measure ocean structure in regions and seasons rarely observed with traditional oceanographic platforms. Over the last few years, seals have allowed for a considerable increase in temperature and salinity profiles from the SO. However we were still lacking information on the spatio-temporal variation of phytoplankton concentration. This information is critical to assess how the biological productivity of the SO, with direct consequences on the amount of CO_2 "fixed" by the biological pump, will respond to global warming. In this research program, we use an innovative sampling fluorescence approach to quantify phytoplankton concentration at sea. For the first time, a low energy consumption fluorometer was added to Argos CTD-SRDL tags, and these novel instruments were deployed on 27 southern elephant seals between 25 December 2007 and the 4 February 2011. As many as 3388 fluorescence profiles associated with temperature and salinity measurements were thereby collected from a vast sector of the Southern Indian Ocean. This paper address the calibration issue of the fluorometer before being deployed on elephant seals and present the first results obtained for the Indian Sector of the Southern Ocean. This in situ system is implemented in synergy with satellite ocean colour radiometry. Satellite-derived data is limited to the surface layer and is restricted over the SO by extensive cloud cover. However, with the addition of these new tags, we're able to assess the 3 dimension distribution of phytoplankton concentration by foraging southern elephant seals. This approach reveals that for the Indian sector of the SO, the surface chlorophyll *a* (chl *a*) concentrations provided by MODIS were underestimated by a factor of the order of

ESSDD
5, 853–891, 2012

2–3 compared to in situ measurements. The scientific outcomes of this program include an improved understanding of both the present state and variability in ocean biology, and the accompanying biogeochemistry, as well as the delivery of real-time and open-access data to scientists (doi:10.7491/MEMO.1).

1 Introduction

Polar marine ecosystems, and in particular the Southern Ocean (SO hereafter), are among the most vulnerable ecosystems to climate change. However there is conflicting evidence on how the biological productivity of these Polar Ocean will respond to global warming. The SO plays an important role in the carbon cycle and it is one of the largest sink for anthropogenic CO_2 through formation of deep water around Antarctica and intermediate water in the vicinity of the subantarctic zone (Caldeira et al., 2000; LoMonaco et al., 2005). Furthermore, by contributing to roughly half of the biosphere's primary production, photosynthesis by oceanic phytoplankton is a vital link between living and inorganic stocks of carbon (Field et al., 1998; Berhenfeld et al., 2006). However our understanding of the variability of SO's primary productivity is hampered by the lack of in situ observations available for this logistically difficult region, and much of the existing observations are heavily biased towards the austral summer.

However, the degree of confidence for primary production derived from satellite-based estimates of phytoplankton biomass is still debated. This is especially true in SO, where satellite measurements tend to under-estimate chl *a* concentrations (Dierssen and Smith, 2000; Holm Hansen et al., 2004; Garcia et al., 2005; Dierssen, 2010; Kahru and Mitchell, 2010). There is growing evidences of the limitations of satellite assessments of primary production. Satellites scan the sea surface, however they are not able to provide subsurface chlorophyll profiles. Deep fluorescence maxima have been found within the frontal zone of the Antarctic Circum Current (ACC hereafter, Queguiner and Brzezinski, 2002; Holm-Hansen et al., 2004) or in the vicinity of the ice edge (Waite and Nodder, 2001). Persistent cloud cover and fragmented sea-ice also constitute towards

ESSDD
5, 853–891, 2012

major limitation of satellite ocean colour measurements in the SO (Arrigo et al., 1998; Buesseler et al., 2003).

Evaluation of the distribution of chl *a* throughout the water column is one of the most important biological parameters in the ocean because it is an indicator of the spatial and temporal variability of primary productivity (Behrenfeld and Falkowski, 1997). As a consequence, to complement remotely sensed ocean colour data, year-round surveys of the in situ optics as well as the physical oceanographic measurements is required for a description of spatial (horizontal and vertical) and temporal (seasonal, inter-annual) distribution of phytoplankton. In turn, this data will contribute to our understanding of how primary production within SO may respond to climatic changes.

Subsurface chl *a* measurements are traditionally performed from research vessels, using profiling fluorometers and water samples collected by Niskin bottles. Alternatively, chl *a* profiles can be obtained from fluorometers deployed on fixed moorings or autonomous platforms like Argo floats (Roemmich et al., 2004), or autonomous underwater vehicles (Yu et al., 2002). Rapid technological advances in ocean observation have nevertheless been achieved during the last decade, particularly with respect to physical climate variables. Developing such in situ observation systems is an essential step towards a better understanding of biogeochemical cycles and ecosystem dynamics, especially at spatial and temporal scales that have been unexplored until now. However, with regard the carbon cycle, establishment of in situ observing systems in the under-sampled SO remains challenging due to its remoteness, harsh weather conditions and the presence of sea-ice.

Here we present the development of an original synergy between biologist's efforts to understand the marine life of top predators, and physical and biogeochemical oceanographic studies through development of new bio-logging devices deployed on southern elephant seals (*Mirounga Leonina*), SES hereafter. This device incorporates high accuracy temperature and salinity sensors, as well as a fluorometer and provides a range of new behavioural and physiological data on free ranging marine animals for biologists, while simultaneously gathering vertical profiles of temperature, salinity and

ESSDD
5, 853–891, 2012

fluorescence for oceanographers. Profiles sampled in the remote SO are of great interest as they can fill a niche within the ocean observing system, where such measurements are lacking (e.g. Charrassin et al., 2008; Nicholls et al., 2008; Roquet et al., 2009; Wunch et al., 2009). One important aspect of this methodology is the near real-time delivery of CTD-Fluo profiles using the Argos satellite system (Argos, 1996). SESs provide an ideal "plateform" for such investigation as they dive nearly continuously and at great depths (Hindell et al., 1991). Moreover, they undertake long foraging trips each year, exploring large areas of the SO (Biuw et al., 2007).

However to make most of the use of these fluorescence data it is essential to develop effective means for calibration, quality control, and postprocessing to provide consistent data set to oceanographers and for climatologies. Therefore the first objective of this paper is to report the calibration and the profile qualification procedure on a unique 2-yr fluorescence dataset collected by southern elephant seals (SES hereafter) within the Indian sector of the Southern Ocean. From this data we will assess how in situ measurements compare with surface chl *a* concentration measured by ocean colour satellites. This new approach allows sustained acquisition of chl-*a* fluorescence profiles (proxy for chl-*a* concentration) in areas where data scarcity is the rule and how they complement satellite ocean colour data.

2 Materials and methods

2.1 Instrumentation

A thorough technical description of CTD-SRDLs can be found in Boehme et al. (2009), which we briefly summarize here (see also Fedak et al., 2002). CTD-Fluoro-SRDLs have been designed as miniaturized platforms to record behavioral data and log in situ CTD profiles. They can be deployed on a range of marine mammals (e.g. Lydersen et al., 2002; Boehme et al., 2008; Nicholls et al., 2008; Roquet et al., 2009). The devices contain (1) a Platform Terminal Transmitter (PTT) to transmit compressed data through

ESSDD
5, 853–891, 2012

the Argos satellite system, (2) a micro-controller coordinates the different functions e.g. sensor data acquisition (data processing and transmission based on the internal setup and energy budget, Boehme et al., 2009 and (3) a miniaturized CTD (Valeport LTD, Totnes, UK).

The specifications of the miniaturized CTD (Valeport Ltd, Totnes, UK) result from a trade-off between the need for miniaturization, energy consumption, stability and sensor performance. The pressure measurements are made by a Keller series-PA7 piezoresistive pressure transducer1 (Keller AG, CH) with a given accuracy of better than 1 % of the full-scale reading (±20 dbar at 2000 dbar). However, laboratory experiments have shown a performance of better than 0.25 % of the actual reading (Boehme et al., 2009). The temperature probe is a fast response Platinum Resistance Thermometer (PRT) made by Valeport (range: −5 °C to +35 °C, accuracy: ± 0.005 °C, time constant: 0.7 s) and an inductive conductivity sensor by Valeport (range: 0 to 80 mS cm^{-1}, accuracy: better than ± 0.01 mS cm^{-1}).

Implementation of a fluorometer to estimate chl *a* concentration

In vivo fluorescence F is a widely used technique to estimate chl *a* concentration in aquatic environments and can be expressed as:

$$F = Ea \cdot [\text{chl } a]\varphi_f \quad (1)$$

where E (mole quanta m^{-2} s^{-1}) is the intensity of the exciting source, $a*$ is the chl-specific absorption coefficient (m^2 mg [Chl *a*]$^{-1}$) [Chl *a*] is the chl *a* concentration (mg chl *a* m^{-3}) and φ_f is the quantum yield for fluorescence [(mole of emitted quanta (mole absorbed quanta^{-1})].

The fluorescence-chl *a* relationship for a given fluorometer varies according to environmental conditions such as the phytoplankton taxonomic composition and physiological adaptative mechanisms (e.g. Falkowski and Kolber, 1995; Babin et al., 1996, 2008).

ESSDD
5, 853–891, 2012

The Cyclops 7 is a compact cylinder (110 × 25 mm after removal of the end cap), low energy consumption single channel fuorescence detector that can be used for many different applications. It delivers a voltage output that is proportional to the concentration of the chl *a* particle, or compound of interest. For chl *a* detection a 460 nm exciting wavelength and a 620–715 nm fluorescence detection photodiode are used. According to Turner Design specifications the minimum detection limit is 0.025 $\mu g\,l^{-1}$ of chl *a*. The Cyclops 7 can be set on different level of sensitivity for chl *a* detection allowing detection of maximum chl *a* concentration ranging generally from low (i.e. detection range 0–500 $\mu g\,l^{-1}$) to medium (0–50 $\mu g\,l^{-1}$) and high (0–5 $\mu g\,l^{-1}$) sensitivities. For our application according to [Chl *a*] climatologies available, the initial detection range was set between 0–2.5 $\mu g\,l^{-1}$ a range matching well the chl *a* concentration generally encountered within the SO.

The Cyclops 7 was integrated in a new CTD-Fluo Satellite Relay Data Loggers (Tags hereafter). They were built by the Sea Mammal Research Unit (SMRU) (University of St. Andrews, Scotland). Fluorescence was sampled continuously between the surface and 180 m. As Argos messages are restricted in length we had to reduce the resolution of fluorescence data. Therefore values were averaged for eighteen 10 m vertical sections. For each section the mean fluorescence value was allocated to the mid depth point of the corresponding section.

Fluorometer calibrations, relying essentially on chl *a* solutions or on phytoplankton cultures, are generally provided by manufacturers. Most of the time these calibrations are established for large range of chl *a* concentrations not always representative of in situ ones. Therefore it is highly desirable to confirm or adjust through in situ calibration on natural samples (see Xing et al., 2012). As part of this program a thorough calibration and testing procedure was undertaken for the CTD-Fluo SRDL. Pre-deployment calibrations of the tags and at-sea validating test were conducted prior to SES deployment. This procedure was followed for most deployments in this study. Before being taken into the field, devices were calibrated at Valeport, Service Hydrographique de

ESSDD
5, 853–891, 2012

la Marine (Brest, France), and had temperature (T) and conductivity (C) resolutions of 0.001 °C and 0.002 mS cm^{-1}, respectively (see Roquet et al., 2011 for details).

2.2 Calibration procedure

The fluoremeter were inter-calibrated by implementing a Bayesian procedure using all information available regarding the predeployement test as well as the post-deployment information collected.

2.2.1 Fluorometer inter-calibration and conversion in chl *a* concentration

Pre-deployment tests

Five consecutive sessions of CTD-Fluo SRDL deployments on SES (ft01, ft02, ft03, ft04 and ft06) were conducted as part of this study. The first two tags (ft01) were deployed on a seal without any pre-deployment test. For the second deployment (ft02), 8 tags were tested simultaneously tested at sea at Kerguelen along a 100 m-cast.

For the following deployment (ft03, ft04, ft06) and previous to their operational deployments on SES at Kerguelen Island the tags were tested in the Mediterranean sea during shipboard experiments. At sea-tests were performed during the BOUSSOLE oceanographic cruises on the SSV "Tethys II" (Resp. D. Antoine, LOV). Each cruise consisted of a transect between the Nice harbour and the BOUSSOLE mooring site located in the north western Mediterranean sea (43°20′ N, 7°54′ E) with up to 6 oceanographic casts performed in between (Fig. 1). As part of the BOUSSOLE program and associated cruises (Antoine et al., 2008) in the Ligurian Sea (Western Mediterranean), each series of tag were indeed attached to a CTD rosette generally deployed at Boussole site.

Water samples were collected for 10 different depths, filtered onboard and immediately frozen in liquid nitrogen before being stored at −80 °C back in the laboratory. High Performance Liquid Chromatography (HPLC) analysis of filtered samples was

ESSDD
5, 853–891, 2012

performed according to Ras et al. (2008) for the accurate determination of total chl *a* and accessory pigments (other chlorophylls and carotenoids).

The in-situ calibration procedures for each tag subsequently include the deep offset fluorescence correction. Offset is detected in the profile through the fluorescence value (Fluo) in deep waters (like $z > 200$ m). Chl *a* fluorescence is considered as null at these depths because HPLC [Chl *a*] is below the detection limit (DL) of the method (DL = 0.05 mg m^{-3}). For each tag and each cast, the fluorescence-offset was calculated as difference between 0 and the fluorescence value provided by the fluorometer for every depth greater than 200 m. The mean and standard deviation (SD) of the fluorescence offset was then calculated for each tag. The mean offset value calculated for a given cast and a given fluorometer was retrieved to the fluorescence values provided by this fluorometer. The at-sea test offset calculation for ft02 was restrain between 80 and 100 m, for which fluorescence for all fluorometers reached constant and minimum values which were consistent with the offset values generally found during the other at-sea test.

Only the ascent values were used as (i) the water samples were only collected during the ascent phase and (ii) the CTD-Fluoro SRDL tags were programmed to sample the fluorescence only during the ascent phase when deployed on an elephant seal.

For this calibration procedure, tags were set on a sampling protocol and programmed to record pressure, temperature, conductivity and fluorescence every 2 s continuously while in the water. They were deployed to the side of the water-sampling rosette which was equipped with 11, 12 Niskin bottles (General Oceanics) and a SBE 21 CTD profiler (Seabird Electronics) and with a CHELSEA AquaTrack chl *a* fluorometer (hereafter named reference fluorometer). Chl *a* concentration was determined by HPLC on a sample of 2.27 l of water collected by the Niskin bottles for one and sometime two casts during the cruise. Water samples were usually collected from 12 depths (5, 10, 20, 30, 40, 50, 60, 70, 80, 150, 200 m).

The multiple casts conducted, without water sampling, allow us to (1) assess the deep fluorescence offset for each tag and to assess its inter-cast variability and (2)

ESSDD
5, 853–891, 2012

to assess discrepancies between different fluorometers were consistent among and between casts.

Chl *a* concentrations of the water samples collectected on BOUSSOLE site were determined using standard fluorometric analysis of acetone extracts of the filtered samples. Water samples collected using Niskin bottles were filtered (2250 cm^3) onto glass fiber filters (Whatman GF/F, nominally 0.7 µm) using positive pressure. The filters were placed in a test tube, wrapped in aluminium foil and frozen in the dark. Back in the Villefranche laboratory chl *a* was extracted from the filter with 7 ml of HPLC grade acetone for 24 h in the dark. The pigment concentration was then analyzed by the fluorometric method (Yentsch and Menzel, 1963) with a blanked and calibrated fluorometer (Turner Designs 10-AU).

Despite the off-set correction and a good agreement in the general shape of the fluorescence profiles provided by each fluorometer for a given cast, differences in absolute fluorescence values are clearly noticeable between fluorometers (see Fig. 2) which means that the calibration parameters provided by the manufacturer were not precise enough and/or that the integration of the fluorometer into the CTD SRDL tag degraded the fluorometer calibration. Therefore the fluorometers of the CTD-Fluo tags needed to be re-calibrated in situ again.

To do so, for a given cast, offset corrected fluorescence values, the regression coefficient was calculated (without constant) for depth ranging between 0 and 200 m between the offset corrected fluorescence values provided by each CTD-Fluo SRDL tested and the corresponding fluorescence values provided by the reference fluorometer for (ft03/ft04 and ft06). Several casts were conducted for a given at-sea test allowing to estimate intra and inter-fluorometer variability.

Post-deployment procedure

The second step was to proceed to the inter-calibration of the fluorometers between all the at-sea tests and this was essential for the ft01 and ft02 for which no proper at complete at sea calibration procedure was performed previous to seal deployment. For

ESSDD
5, 853–891, 2012

ft02, the simultaneous testing of all the tags provided information about the proportionality between the fluorescence measurements provided by the different fluorometers and that information was used.

To intercalibrate the tags between each deployment we used all the information provided by at sea tests as well as the proportionality found between surface values provided by the tag fluorometer within a deployment and the corresponding chl *a* surface values provided by MODIS. 8-day composite 9 km scale resolution MODIS data was the highest usable resolution to investigate the relationship between in situ surface fluorescence chl *a* and those provided by MODIS. Indeed too few MODIS values were available to investigate this relationship at a higher temporal (daily) and spatial (1 km) resolution at the tag level. The tag's surface fluorescence values used were offset and quenching corrected and saturated values retrieved (see below). The coefficient found between the MODIS surface fluorescence values for each deployment was used to proceed to the production of a homogeneous fluorescence data set.

Conversion to chl *a* concentration

The inter-calibrated fluorescence values were then converted into a chl *a* concentration ([Chl *a*] hereafter) value by using the relationship between the chl *a* concentration provided by the reference fluorometer and the [Chl *a*] provided from HPLC measurements. This relationship was estimated over 70 test profiles ranging between 0 to 200 m and performed between 2002 and 2009. As all these profiles were performed during daylight hours, therefore only fluorescence values deeper than 30 m were used to avoid any quenching effect and fluorescence values provided by the reference fluorometer were offset corrected.

2.2.2 Deployment on elephant seals

Instruments were deployed on SES either at the end of their moult in late summer to cover their pre-breeding, winter foraging trips or in October on post-breeding females.

ESSDD
5, 853–891, 2012

Animals were anesthetized with intravenous injection of tiletamine and zolazepam 1 : 1, and then instruments were attached to the fur on their head by using a two component industrial epoxy. Seals dove repeatedly with CTD-Fluo data being collected every 2 s during the ascent phase of dive and processed onboard before being transmitted via the Argos satellite system when animals were at the surface. On average, 1.8 ± 0.5 vertical temperature (T), conductivity (C) and fluorescence profiles were transmitted daily. Because of the narrow bandwidth of Argos transmitters, each profile was transmitted in a compressed form consisting of 18 fluorescence and 24 Temperature (T) and Conductivity (C) data points. The 18 first T and C corresponded to the fluorescence measurements for the 0–180 m depth range. Fluorescence, T and C measurements were averaged over 10 m bin sampled for the upper 180 m of the dive. The 6 additional T and C corresponded to the most important inflection points determined onboard over between 180 m – and the deepest part of the dive by using a "broken stick algorithm" (Roquet et al., 2011).

2.2.3 Post deployment issues and correction processes

Chl *a* saturated values

According to chl *a* measurements available for the study area ft02, ft03, ft04 CTD-Fluoro SRDL Tags the Cyclops 7 fluorometer gain was set to monitor chl *a* concentration ranging between 0 and 2.5 $\mu g\,l^{-1}$. In situation of high in situ chl *a* concentration, some raw profiles exhibited saturated values. Therefore these profiles were flagged accordingly and retained as saturated one in the data base. For the ft06 Tags the gain of the Cyclops 7 fluorometer was set for a dynamical range of 0 to 4 $\mu g\,l^{-1}$ and saturated chl *a* profiles were exceptionally encountered and flagged accordingly. Unsaturated profiles were flagged as "1" while saturated profiles were flagged as "2".

ESSDD
5, 853–891, 2012

Offset correction

Initially each in situ profiles was corrected according to the mean offset calculated for each tag from the at sea test conducted prior to deployments which exhibited very little variability for a given fluorometer between cast (see result part). However post deployment values revealed that this offset could vary over time, and the reasons for such variations are not yet fully understood but are thought to be related to the water masses encountered and in particular the amount of non phytoplanktonic particles. The use of a constant offset correction was leading to positively or negatively bias profiles values depending on situations. Therefore, a profile-by-profile-offset-correction method was implemented and three cases were distinguished and flagged accordingly. In the first situation the 4 deepest chl *a* values corresponded (i) to the minimum values of the profiles, with a standard deviation (SD) on chl *a* value lower than 10 %. In this situation the lowest chl *a* value among the 4 deepest values was used as the offset value and the whole profile was corrected and flagged as "1"; (ii) when the deepest chl *a* values did not correspond to the minimum values, or when the CV was higher than 10 % the profile was flagged as "2" and was corrected according to the mean offset calculated for that Tag over the whole deployment period; (iii) a third situation was observed in a few cases, and for which chl *a* concentration was increasing at depth. No offset correction was applied to these profiles which were flagged as "3" these flag 3 profiles are not integrated in the current data base.

Quenching correction

In both, laboratory and field studies, a daily rhythm of in vivo fluorescence that is not correlated with diel changes in the concentration of chl *a* have been reported in a number of studies. During periods of high irradiance, fluorescence tends to be lower than the value at night (Kiefer, 1973; Loftus and Seliger, 1975; Falkowski and Kolber, 1995; Dandonneau and Neveux, 1997; Behrenfeld and Kolber, 1999; Kinkade et al., 1999). The photo-inhibition of phytoplankton by an excess of light, result in a decrease

ESSDD
5, 853–891, 2012

of the fluorescence quantum yield (i.e. the ratio of photons emitted as fluorescence to those absorbed by photosynthetic pigments). This is often ascribed to a set of processes generally termed non-photochemical fluorescence quenching (NPQ; Falkowski and Kolber, 1995; Krause and Jahns, 2004). Quenching is commonly observed during daytime with a maximum intensity at midday (Kiefer, 1973; Dandonneau and Neveux, 1997) and it is refer as daytime fluorescence quenching. Quenching poses a problem and therefore need to be accounted for. We applied the new method of quenching correction developed, tested and successfully applied to fluorescence data collected by elephant seals (Xing et al., 2012). In short, for mixed type waters, the maximum fluorescence values within the mixed layer is extended to the surface, (i.e. all upper points are replaced by this maximum value). However, for stratified waters, which usually have a thin mixed layer, obviously, the quenching effect will pass through the mixed layer into the stratified layer. In the stratified layer we were unable to perform such correction and only night time fluorescence profiles were used. However, the stratified layer situations was only encounter for 16 % of the fluorescence profiles sampled, and nearly half of then were obtained at night. In this process, we assume the maximum value in the mixed layer as the non-quenching value and all above points are corrected to the same value (see Xing et al., 2012). After implementing such corrections, no differences could be detected between day time fluorescence corrected profiles and the proximate night profiles (just before or after the day profiles).

2.2.4 Estimation of the tag specific chl *a* correction coefficient: a Bayesian approach

Using a Bayesian adjustment framework, and by combining for each at sea test the information available for each profiles and the HPLC values available, a chl *a* calibration coefficient was calculated for each CTD-Fluoro SRDL tags. A Bayesian framework is especially suited as it guarantees that between-casts variability is taken into account in estimating these inter-fluorometer coefficients. An attractive feature of this framework is the relative ease with which different data sets are combined in a single

ESSDD
5, 853–891, 2012

analysis, allowing information transfer between disparate sources. Another advantage stems from the easy computation of confidence intervals for parameters of interest and prediction errors. Models were fitted with *WinBUGS* (Spiegelhalter et al., 2003) called from *R* (R Development Core Team, 2009) with the package *R2WinBUGS* (Sturtz et al., 2005). Weakly informative and robust priors were favoured. We used uniform priors (Gelman, 2006) for standard deviation parameters. Because all slopes were expected to be positive, we used Student-t priors with mean 0, scale 10 and 7 df on a log scale (Gelman et al., 2008). Batches of tag-specific coefficient were assumed to follow a bivariate Gaussian distribution with covariance matrix $\sum$. We used the prior described in Tokuda et al. (2011) for the covariance matrix $\sum$.

We built a model to predict HPLC [Chl *a*] from either in situ fluorescence (Fluo) at measured by instrumented SES, or from MODIS chl. Specifically we first used long-term data at the Boussole site to estimate the relationship between HPLC [Chl *a*] and measurement from the reference fluorometer:

$$\text{HPLC [Chl } a\text{]} = \delta \cdot \text{Fluo[reference]} + \varepsilon 1 \quad (2)$$

where $\varepsilon 1$ is a Gaussian residual error term.

Secondly, we used data from the intercalibration experiment to estimate the relationship between a specific tag j and the reference fluorometer:

$$\text{Fluo[reference]} = \alpha j \cdot (\text{Fluo } j - \text{Offset } j) + \varepsilon 2 \quad (3)$$

where $\varepsilon 2$ is a Gaussian residual error term. When measurements from the reference fluorometer were unavailable but measurements from the different tags at a specific location were available, we rewrote Eq. (3) as:

$$\text{Fluo[reference]} - \alpha j \cdot (\text{Fluo } j - \text{Offset } j) + \varepsilon 2 = 0 \quad (4)$$

and put a weakly informative prior (Half-Student-t with mean 0, scale 5 and 4 df, Gelman et al., 2008) on the value of Fluo[reference]. We then used the *WinBUGS* "zero-trick" (Spiegelhalter et al., 2003) to incorporate these data into the model. Note that the error term $\varepsilon 2$ is the same for Eqs. (3) and (4).

ESSDD
5, 853–891, 2012

Finally, we evaluated the relationship between in situ fluorescence as measured from a specific tag j and MODIS:

$$(\text{Fluo } j - \text{Offset } j) = \beta j \cdot \text{MODIS} + \varepsilon 3 \quad (5)$$

where $\varepsilon 3$ is a Student residual error term. Equation (5) is a regression with heteroskedastic noise to account for possible outliers, or extreme observations, when evaluating the relationship between MODIS and in situ fluorescence. To make robust inferences, the parameter ν, that is the degrees of freedom of the Student distribution, was estimated from the data (with a Gamma (shape = 2, scale = 4) prior for ν).

Combining Eqs. (2) and (3) yields:

$$\text{HPLC [Chl } a] = \delta \cdot \text{Fluo[reference]} = \delta \cdot \alpha j \cdot (\text{Fluo } j - \text{Offset } j) \quad (6)$$

where $\delta \cdot \alpha j$ is a tag specific calibration coefficient allowing to predict HPLC [Chl a] from in situ fluorescence. Combining Eqs. (5) and (6) further yields:

$$\text{HPLC [Chl } a] = \delta \cdot \alpha j \cdot \beta j \cdot \text{MODIS} \quad (7)$$

which allows to predict for each tag the likely value of HPLC [Chl a] from MODIS measurement.

3 Results

3.1 At-sea trials prior to deployment

The at-sea testing previous to deployment revealed two types of issues which were tag's fluorometer dependant: (1) a fluorescence offset was observed and therefore an instrument-specific clean water background, equivalent to the lowest values observed in the deepest part of the fluorescence profiles was subtracted from the raw fluorescence values; (2) for offset-corrected fluorescence profile, differences between tags in the absolute amount of fluorescence were detected.

ESSDD
5, 853–891, 2012

The variability of the fluorescence offset for a given tag was one order of magnitude smaller than the offset differences between tags (Table 1). The mean fluorescent offset for the tested tags during the BOUSSOLE cruise was $0.24 \pm 0.05\,\mu g\,l^{-1}$ (range 0.16–0.33, $n = 14$). For a given tag, the standard deviation of inter-cast fluorescent offset ranged from (0.0007 to 0.0620, mean = $0.0148\,\mu g\,l^{-1}$).

3.1.1 Tag's fluorometer intercalibration

The multiple cast performed during the at sea test prior to ft03, ft04 and ft06 deployments allowed assessing the intra tag-fluorometer variability. This variability ranged from to a minimum of 0.03 % to a maximum of 5.61 % with a mean of 2.08 ± 1.84 %. However, the difference between fluorometers was one order of magnitude larger than the within fluorometer variability and one fluoromenter provided fluorescence values which were on average 2.61 time higher than the minimal values. The mean inter-fluorometer variation in fluorescence values was 69 % (range 0.005 to 261 %).

3.1.2 Reference fluorometer-HPLC relationship

Over the 2002–2009 period, HPLC values were found to be linearly related to the chl *a* estimates provided by the reference fluoremeter. δ was estimated to be 2.53 (i.e. [Chl *a*] concentration provided by HPLC were found to be 2.53 higher than those estimated from the reference fluorometer (Fig. 3, Table 1).

3.2 Post deployment data

From December 2007 to July 2010, a total of 27 SES, were fitted tags, of which 23 provided usable fluorescence data (Table 1). The 23 SES tracks provided a broad geographic and seasonal coverage ranging from Antarctic to subtropical waters, but with most individuals concentrating east of Kerguelen Island within the Kerguelen plume (Fig. 4). A total of 4662 fluorescence profiles were transmitted, but 1274 of them either incomplete, with constant values or presenting obvious anomalies were discarded

ESSDD
5, 853–891, 2012

(i.e. 27 %). Among the remaining 3388 profiles 1776 were collected during the day and 1612 at night and year round (Fig. 5). The summary of the different profiles and flagging situation are provided in Table 1. This data set (doi:10.7491/MEMO.1) is freely available at http://www.cebc.cnrs.fr/ecomm/Fr_ecomm/ecomm_memoOCfd.html.

524 profiles exhibited saturated fluorescence values (i.e. 18 %) and were excluded for the comparison with the corresponding weekly Chl *a* MODIS data. However due to heavy cloud cover only 884 surface values of CTD-fluo profiles (i.e. 30.9 %) could be matched with the weekly MODIS data, and only 126 with the MODIS data collected on the same day (i.e. 4.4 %).

Among these 23 tags deployed on SES, 8 were recovered when SES came back onshore after at sea periods ranging between 3 to 8 months. At recovery the optical face of Cyclops 7 was clean with no bio-fouling most likely because elephant seals are typically deep divers spending very short periods within the euphotic zone. Furthermore they spent most time at low temperatures.

On the 3388 fluorescence profiles, 40 % exhibited day time fluorescence quenching (i.e. 70 % of daytime profiles-table 1). Therefore these profiles were corrected according to the procedure proposed by (Xing et al., 2012). The recovery of fluorescence from quenching is obvious when we compare day profiles with night profiles obtained for the same location at the same date (Fig. 6). Individual seal collected chl *a* transects along their track monitoring latitudinal/longitudinal changes for a given time period as well as seasonal change within a given area (Fig. 7).

As quenching could only be corrected in well mixed water and not in stratified ones, we were (1) unable to proceed to quenching correction of fluorescence profiles in 283 profiles (i.e. about 16 % of the day profiles) and therefore unable to assess properly deep maximum fluorescence for day time fluorescence profiles. To address this question we only used the 1612 night profiles. Among those 352 had a maximum value at surface, while 742 exhibited a maximum deeper than 30 m. However the vast majority the maxima was not exceeding the surface values by more than 30 % (i.e. 1423 profiles). Only 148 night profiles (i.e. 9 % of the total number of night profiles) had a deep

ESSDD
5, 853–891, 2012

maximum exceeding 30 % of the surface value (maximum: 180 %). The depth class distribution of the maxima values exceeding 30 % of the surface value are shown in Fig. 8 and exhibit a clear bimodal distribution with a 30–40 m and a 70–80 m modes.

No obvious spatial structuring in the distribution of these profiles could be identified through the range of the SES.

Surface fluorescence values obtained from deep offset and quenching corrected profiles provided by intercalibrated tags according to the reference fluorometer (ft03, ft04 and ft06) and were related to the corresponding MODIS chl *a* value. This relationship was implemented within the Bayesian framework to correct tag fluorescence values for which no at sea test was performed previous to the deployment. For the ft02 deployment the proportionality found between tags, all tested simultaneously at sea. Following the Bayesian procedure previously described the correction coefficients ($\delta \cdot \alpha j$, mean value) applied to each tag were calculated and are given in Table 2.

The surface [Chl *a*] values derivated from by offset and quenching corrected profiles were found to be related to the 8-day-9 km MODIS chl *a* values. However we found that on average, MODIS tended to underestimate [Chl *a*] by a mean 1.99 factor ($\delta \cdot \alpha j \cdot \beta j$) compared to the in situ estimates provided by the calibrated fluorescence tag (Table 2, Fig. 9). For the Southern Ocean total absence of chl *a* was never detected by MODIS with the lowest value observed of 0.06 $\mu g\, l^{-1}$ in our case, while in situ fluorescence measurements suggest that total absence of chl *a* can be observed.

4 Discussion and conclusion

The fluorescence profiles collected by the SES within the SO, provides 3-D information on otherwise poorly sampled area such as the Antarctic sea-ice zone, an area were the ocean satellites are blinded by sea-ice and/or cloud cover. SES, provided an unequalled data set of fluorescence profiles associated with temperature and salinity measurements (i.e. density) for a broad sector of the Indian part of the SO and this data

ESSDD
5, 853–891, 2012

set represents a significant contribution in to understanding of the seasonal variation of phytoplankton biomass.

The significant contribution of this study was to propose a detailed and step by step procedure to intercalibrate the fluorometer to provide consistent chl *a* estimates. To summarize the first step requires the correction of the deep fluorescence offset, the second step requires to have at least a common reference fluorometers between the performed tests. The third step, i.e. to proceed to the HPLC calibration, requires eliminating quenching affected fluorescence surface values obtained during daytime or better to perform night fluorescence profiles. Furthermore, we suggest that this HPLC intercalibration should not to be performed on profile to profile basis but instead according to the fluorescence/ chl *a* relationship established from multiple at-sea tests. We found in this study that while the fluorescence-HPLC chl *a* relationship can vary from one at-sea test to the other, however the long term relationship established over several years and encompassing numerous at-sea test exhibit a very good linear relationship (Fig. 3). Therefore we suggest using this global relationship to transform the inter-calibrated fluorescence values provided by the fluorometers to an actual estimation of [Chl *a*] value. In a last step when they are sufficient surface fluorescence measurements coinciding with MODIS one, MODIS data can be used as a common but weak relative (not absolute) reference between fluorometers.

One important result of this study was to show that MODIS may underestimate surface chl *a* by a 2 to 3 factor depending on the in situ concentration (Fig. 9). In-situ chl *a* concentration provided by the fluorometer was weekly correlated with the MODIS. Data points were highly dispersed, but this is not surprising due to the low spatial and temporal resolution of the MODIS data used to investigate this relationship while surface values collected by the tags were associated with a unique location within that 9 × 9 km sector and therefore small scale variation which can be measured by the fluorometer are likely to be overlooked by the 9 × 9 km MODIS and weekly data.

This finding is consistent with several studies showing that standard satellite ocean colour algorithms tend to underestimate chl *a* concentrations in the SO compared to

ESSDD
5, 853–891, 2012

in situ HPLC measurement or from calibrated fluorometer (Mitchell and Holm-Hansen, 1991; Dierssen and Smith, 2000; Holm-Hansen et al., 2004; Garcia et al., 2005) with standard algorithms typically underestimating chl *a* by 2–3 times (Kahru and Mitchell, 2010) and consistent with our study, and up to 5 times (Dierssen, 2010). These errors are typically transferred to the estimates of primary production and carbon fluxes.

Therefore we are confident that the current MODIS data underestimate by a large extent the in situ [Chl *a*]. In our study the MODIS underestimation was found over the whole study area and therefore encompassed a broad range of phytoplankton assemblage. But future studies should investigate in greater details if the relationships between chl *a* surface concentration estimated from in situ fluorescence measurements and MODIS do vary according to the biogeographic regions of the SO visited by the SES.

Global estimates of ocean primary production are now based on satellite Ocean Colour data (Longuhurst et al., 1995; Antoine et al., 1996; Behrenfeld and Falkowski, 1997; Behrenfeld et al., 2005). Time series have been built, from which climate-relevant trends can be extracted (Antoine et al., 2005; Polovina et al., 2008; Martinez et al., 2009). In situ and satellite data are highly complementary. Whereas in situ data extend the satellite information into the ocean interior (unseen by the remote sensor) and provide indispensable sea truth data, satellite provides the synoptic coverage.

We also found that when taking into account the quenching effect, deep maxima chl *a* concentration exceeding 30 % of the surface value were found only in 9 % of the night profile. According to this result the decoupling of surface and deep phytoplankton biomass observed for only 9 % of the profiles is unlikely to be a major issue when estimating primary production from surface data. However the real issue is the quenching effect observed during daylight hours and requiring to be properly dealt with (Xing et al., 2012).

Models can only provide useful answers if there are sufficient data to constrain the underlying processes and validate the model output. New approaches to assimilate biological and chemical data into these models are advancing rapidly (Brasseur et al.,

ESSDD
5, 853–891, 2012

2009). Notably, the progressive integration of biogeochemical variables in the next generation of operational oceanography systems is one of the long-term objectives of the GODAE OceanView international program. Nevertheless, and in view of refining these models for improving their representativeness and predictive capabilities, the datasets currently available remain too scarce. There is an obvious and imperative need to reinforce biological and biogeochemical data acquisition and to organize databases and SES equipped with CTD-Fluo SRDL tags are contributing efficiently to this need.

Taking into consideration that in situ acquisition of fluorescence data by SES represent a significant contribution to the observation of the SO to (at least partly) circumvent the issue of undersampling biogeochemical and ecosystem variables within this ocean. These new data implemented in tight synergy with two other essential bricks of an integrated ocean observation system: modelling and satellite observation should represent a significant contribution towards the resolution of important scientific questions relative to the overall phytoplankton biomass and primary production and ultimately changes in carbon fluxes within the SO in relation to climate variability and longer term changes.

Supplementary material related to this article is available online at: http://www.earth-syst-sci-data-discuss.net/5/853/2012/essdd-5-853-2012-supplement.zip.

Acknowledgements. This work was supported by CNES-TOSCA (Southern Elephant sSeal as oceanographer Fluorescence measurements), The MEMO observatory as part of the SOERE CTD-02, the ANR VMC IPSOS-SEAL (2008–2011) and the Total Foundation. We are indebted to IPEV (Institut Polaire Français), for financial and logistical support of Antarctic research program 109 (Seabirds and Marine Mammal Ecology lead by H. Weimerskirch). Special to the BOUSSOLE cruise and team for their help in proceeding at sea tests and to F. Roquet who proceeded to the correction/validation of the temperature/salinity data. Finally we would like to thank all the colleagues and volunteers involved in the field work on southern elephant seals at Kerguelen Island, with the special acknowledgement of the invaluable field contribution of N. ElSkaby, G. Bessigneul, A. Chaigne and Q. Delorme.

ESSDD
5, 853–891, 2012

References

Antoine, D., André, J. M., and Morel, A.: Oceanic primary production 2. Estimation at global scale from satellite (coastal zone color scanner) chlorophyll, Global Biogeochem. Cy., 10, 57–69, 1996.

Antoine, D., Morel, A., Gordon, H. R., Banzon, V. F., and Evans R. H.: Bridging ocean color observations of the 1980s and 2000s in search of long-term trends, J. Geophys. Res., 110, C06009, doi:10.1029/2004JC002620, 2005.

Antoine, D., D'Ortenzio, F., Hooker, S. B., Bécu, G., Gentili, B., Tailliez, D., and Scott, A. J.: Assessment of uncertainty in the ocean reflectance determined by three satellite ocean color sensors (MERIS, SeaWiFS, and MODIS-A) at an offshore site in the Mediterranean Sea., J. Geophys. Res., 113, C07013, doi:101029/102007JC004472, 2008.

Arrigo, K. R., Worthen, D. L., Schnell, A., and Lizotte, M. P.: Primary production in Southern Ocean waters, J. Geophys. Res., 103, 587–600, 1998.

Babin, M., Morel, A., and Gentili, B.: Remote sensing of sea surface sun-induced chlorophyll fluorescence: Consequences of natural variations in the optical characteristics of phytoplankton and the quantum yield of chlorophyll a fluorescence, Int. J. Remote Sens., 17, 2417–2448, 1996.

Babin, M.: Phytoplankton fluorescence: theory, current litterature and in situ measurements, in: Real-time coastal observing systems for marine ecosystem dynamics and harmful algal blooms, edited by: Babin, M., Roesler, C., and Cullen, J. J., 237–280, Unesco, Paris, 2008.

Behrenfeld, M. J. and Falkowski, P. G.: Photosynthetic rates derived from satellite-based chlorophyll concentration, Limnol. Oceanogr., 42, 1–20, 1997.

Behrenfeld, M. J. and Kolber, Z. S.: Widespread iron limitation of phytoplankton in the south Pacific Ocean, Science, 283, 840–843, 1999.

Behrenfeld, M. J., Boss, E., Siegel, D. A., and Shea, D. M.: Carbon-based ocean productivity and phytoplankton physiology from space, Global Biogeochem. Cy., 19, GB1006, doi:10.1029/2004GB002299, 2005.

Behrenfeld, M. J., O'Malley, R. T., Siegel, D. A., McClain, C. R., Sarmiento, J. L., Feldman, G. C., Milligan, A. J., Falkowski, P. G., Letelier, R. M., and Boss, E.,S.: Climate-driven trends in contemporary ocean productivity, Nature, 444, 752–755, 2006.

Biuw, M., Boehme, L., Guinet, C., Hindell, M., Costa, D., Charrassin, J. B., Roquet, F., Bailleul, F., Meredith, M., Thorpe, S., Tremblay, Y., McDonald, B., Park, Y.-H., Rintoul, S., Bindoff,

ESSDD
5, 853–891, 2012

N., Goebel, M., Crocker, D., Lovell, P., Nicholson, J., Monks, F., and Fedak, M.: Variations in behaviour and condition of a Southern Ocean top predator in relation to in-situ oceanographic conditions, P. Natl. Acad. Sci., 104, 13705–13710, 2007.

Boehme, L., Meredith, M. P., Thorpe, S. E., Biuw, M., and Fedak, M.: The Antarctic Circumpolar Current frontal system in the South Atlantic: Monitoring using merged Argo and animal-borne sensor data, J. Geophys. Res., 113, C09012, doi:10.1029/2007JC004647, 2008.

Boehme, L., Lovell, P., Biuw, M., Roquet, F., Nicholson, J., Thorpe, S. E., Meredith, M. P., and Fedak, M.: Technical Note: Animal-borne CTD-Satellite Relay Data Loggers for real-time oceanographic data collection, Ocean Sci., 5, 685–695, doi:10.5194/os-5-685-2009, 2009.

Brasseur, P., Gruber, N., Barciela, R., Brander, K., Doron, M., El Moussaoui, A., Hobday, A. J., Huret, M., Kremeur, A.-S., Lehodey, P., Matear, R., Moulin, C., Murtugudde, R., Senina, I., and Svendsen, E.: Integrating Biogeochemistry and Ecology Into Ocean Data Assimilation Systems, Oceanography, 22, 206–215, 2009.

Buesseler, K. O., Barber, R. T., Dickson, M. L., Hiscock, M. R., Moore, J. K., and Sambrotto, R. N.: The effect of marginal ice-edge dynamics on production and export in the Southern Ocean along 170-W, Deep Sea Res. II, 50, 579–603, 2003.

Caldeira, K., Hoffert, M. I., and Jain, A.: Simple ocean carbon cycle models, in: The Carbon Cycle, edited by: Wigley, T. M. L. and Schimel, D. S., Cambridge University Press, Cambridge, United Kingdom, 199–211, 2000.

Charrassin, J. B., Hindell, M., Rintoul, S. R., Roquet, F., Sokolov, S., Biuw, M., Costa, D., Boehme, L., Lovell, P., Coleman, R., Timmermann, R., Meijers, A., Meredith, M., Park Y.-H., Bailleul, F., Goebel, M., Tremblay, Y., Bost, C.-A., McMahon, C. R., Field, I. C., Fedak, M. A., and Guinet, C.: Southern ocean frontal structure and sea-ice formation rates revealed by elephant seals, P. Natl. Acad. Sci., 105, 11634–11639, 2008.

Dandonneau, Y. and Neveux, J.: Diel variations of in-vivo fluorescence in the eastern equatorial Pacific an unvarying pattern, Deep-Sea Res., 44, 1869–1880, 1997.

Dierssen, H. M.: Perspective on empirical approaches for ocean color remote sensing of chlorophyll in a changing climate, P. Natl. Acad. Sci., 107, 17073–17078, 2010.

Dierssen, H. M. and Smith, R. C.: Bio-optical properties and remote sensing ocean color algorithms for Antarctic Peninsula waters, J. Geophys. Res., 105, 26301–26312, 2000.

Falkowski P. G. and Kolber, Z.: Variations in chlorophyll fluorescence yields in phytoplankton in the world oceans, Aust. J. Plant Physiol., 22, 341–355, 1995.

ESSDD
5, 853–891, 2012

Fedak, M., Lovell, P., McConnell, B., and Hunter, C.: Overcoming the Constraints of Long Range Radio Telemetry from Animals: Getting More Useful Data from Smaller Packages, Integr. Comp. Biol., 42, 3–10, doi:10.1093/icb/42.1.3, 2002.

Field, C. B., Behrenfeld, M. J., Randerson, J. T., and Falkowski, P. G.: Primary production of the biosphere: Integrating terrestrial and oceanic components, Science, 281, 237–240, 1998.

Garcia, C. A. E., Garcia, V. M. T., and McClain, C. R.: Evaluation of SeaWiFS chlorophyll algorithms in the Southwestern Atlantic and Southern Oceans, Remote Sens. Environ., 95, 125–137, 2005.

Gelman, A.: Prior Distributions for Variance Parameters in Hierarchical Models (Comment on Article by Browne and Draper), Bayesian Analysis, 1, 515–534, 2006.

Gelman, A., Jakulin, A., Grazia Pittau, M., and Su, Y.-S.: A Weakly Informative Default Prior Distribution for Logistic and Other Regression Models, The Annals of Applied Statistics, 2, 1360–1383, 2008.

Hindell, M., Slip, D., and Burton, H.: The diving behaviour of adult male and female southern elephant seals, *Mirounga leonina* (Pinnipedia: Phocidae), Aust. J. Zool., 39, 595–619, 1991.

Holm-Hansen, O., Kahru, M., Hewes, C. D., Kawaguchi, S., Kameda, T., Sushin, V. A., Krasovski, I., Priddle, J., Korb, R., Hewitt, R. P., and Mitchell, B. G.: Temporal and spatial distribution of chlorophyll *a* in surface waters of the Scotia Sea as determined by both shipboard measurements and from satellite data, Deep-Sea Res. II, 51, 1323–1331, 2004.

Kahru, M. and Mitchell, G. B.: Blending of ocean colour algorithms applied to the Southern Ocean, Remote Sens. Lett., 1, 119–124, 2010.

Kiefer, D. A.: Fluoresence properties of natural phytoplankton populations, Mar. Biol., 22, 263–269, 1973.

Kinkade, C. S., Marra, J., Dickey, T. D., Langdon, C., Sigurdson, D. E., and Weller, R.: Diel bio-optical variability observed from moored sensors in the Arabian Sea, Deep-Sea Res. II, 46, 1813–1831, 1999.

Krause G. H. and Jahns, P.: Non-photochemical energy dissipation determined by chlorophyll fluorescence quenching: characterization and function, in: Chlorophyll *a* Fluorescence: A Signature of Photosynthesis, edited by: Papageorgiou G. C. and Govindjee, 463–495, Springer, Dordorecht, The Netherlands, 2004.

Lo Monaco, C., Goyet, C., Metzl, N., Poisson, A., and Touratier, F.: Distribution and inventory of anthropogenic CO_2 in the Southern Ocean: Comparison of three data-based methods, J. Geophys. Res., 110, C09S02, doi:10.1029/2004JC002571, 2005.

ESSDD
5, 853–891, 2012

Loftus, M. E. and Seliger, H.: Some limitations of the in vivo fluorescence technique, Chesapeake Sci., 16, 79–92, 1975.
Longhurst, A., Sathyendranath, S., Platt, T., and Caverhill, C.: An estimate of global primary production in the ocean from satellite radiometer data, J. Plankton Res., 17, 1245–1271, 1995.
Lydersen, C., Nøst, O. A., Lovell, P., McConnell, B. J., Gammelsrød, T., Hunter, C., Fedak, M. A., and Kovacs, K. M.: Salinity and temperature structure of a freezing Arctic fjord monitored by white whales (Delphinapterus leucas), Geophys. Res. Lett., 29, 2119, doi:10.1029/2002GL015462, 2002.
Martinez, E., Antoine, D., D'Ortenzio, F., and Gentili, B.: Climate-driven basin-scale decadal oscillations of oceanic phytoplankton, Science, 36, 1253–1256, 2009.
Nicholls, K. W., Boehme, L., Biuw, M., and Fedak, M. A.: Wintertime ocean conditions over the southern Weddell Sea continental shelf, Antarctica, Geophys. Res. Lett., 35, L21605, doi:10.1029/2008GL035742, 2008.
Polovina, J. J., Howell, E. A., and Abecassis, M.: Ocean's least productive waters are expanding, Geophys. Res. Lett., 35, L03618, doi:10.1029/2007GL031745, 2008.
Quéguiner, B. and Brzezinski, M. A.: Biogenic silica production rates and particulate organic matter distribution in the Atlantic sector of the Southern Ocean during austral spring, Deep Sea Res. II, 49, 1765–1786, 2002.
R Development Core Team =R: A Language and Environment for Statistical Computing, R Foundation for Statistical Computing, Vienna, Austria, ISBN 3-900051-07-0, 2002.
Ras, J., Claustre, H., and Uitz, J.: Spatial variability of phytoplankton pigment distributions in the Subtropical South Pacific Ocean: comparison between in situ and predicted data, Biogeosciences, 5, 353–369, doi:10.5194/bg-5-353-2008, 2008.
Roemmich, D., Riser, S., Davis, R., and Desaubies, Y.: Autonomous profiling floats: Workhorse for broad-scale ocean observations, Mar. Technol. Soc. J., 38, 31–39, 2004.
Roquet, F., Park, Y. H., Guinet, C., and Charrassin, J. B.: Observations of the Fawn Trough Current over the Kerguelen Plateau from instrumented elephant seals, J. Mar. Syst., 78, 377–393, 2009.
Roquet, F., Charrassin, J. B., Marchand, S., Boehme, L., Fedak, M., Reverdin, G., and Guinet, C.: Validation of hydrographic data obtained from animal-borne satellite-relay data loggers, J. Atmos. Ocean Tech., 28, 787–801, 2011.
Spiegelhalter, D., Best, T., Best, N., and Lunn, D.: Winbugs user manual version 1.4., 2003.

ESSDD
5, 853–891, 2012

Sturtz, S., Ligges, U., and Gelman, A.: R2winbugs: a Package for Running *WinBUGS* from *R*, J. Stat. Softw., 12, 1–16, 2005.

Tokuda, T., Goodrich, B., Van Mechelen, I., Gelman, A., and Tuerlinckx, F.: Visualizing Distributions of Covariance Matrices, Technical report, University of Leuwen, Belgium and Columbia University, USA, available at: http://www.stat.columbia.edu/~gelman/research/unpublished/Visualization.pdf, 2011.

Waite, A. M. and Nodder, S. D.: The effect of in situ iron addition on the sinking rates and export flux of Southern Ocean diatoms, Deep-Sea Res. II, 48, 2635–2654, 2001.

Wunsch, C., Heimbach, P., Ponte, R., Fukumori, I., and the ECCO-Consortium members: The global general circulation of the oceans estimated by the ECCO-Consortium, Oceanography, 22, 89–103, 2009.

Xing, X., Claustre, H., Blain, S., D'Ortenzio, F., Antoine, D., Ras, J., and Guinet C.: Quenching correction for in vivo chlorophyll fluorescence measured by instrumented elephant seals in the Kerguelen region (Southern Ocean), Limnol. Oceanogr. Method, 10, 483–495, 2012.

Yentz, C. S. and Menzel, D. W.: A method for the determination of phytoplankton chlorophyll and phaeophytin by fluorescence, Deep-Sea Res., 10, 221–231, 1963.

Yu, X., Dickey, T., Bellingham, J., Manov, D., and Streitlien, K.: The application of autonomous underwater vehicles for interdisciplinary measurements in Massachusettsand Cape Cod Bays, Cont. Shelf Res., 22, 2225–2245, 2002.

ESSDD

5, 853–891, 2012

Table 1. Details of the 23 CTD-fluo tags deployments. Deployment date, Sampling period, number of fluoro-profiles obtained, and correction coefficient applied to each tag.

Deployment number	CTD-Fluo SRDL number	Deployment date	End transmission	number of fluorescence profiles collected	number of fluorescence profiles usable	Daylight hours profile	night hours profile	nb of saturated profile	nb of quenching corrected profile	nb prof flag 1 offset profile	nb of prof flag 2 offset profile	Mean offset (predeployment sea test)
FT01	10863	22/12/2007	05/06/2008	241	241	166	75	32	76	212	29	–
FT02	10946	20/01/2009	20/12/2009	331	331	187	144	1	145	248	83	1.28
FT02	11034	20/01/2009	12/03/2009	73	73	45	28	0	15	40	33	0.36
FT02	11035	28/01/2009	21/09/2009	404	404	202	202	0	148	292	112	0.44
FT02	11039	25/01/2009	13/07/2009	289	289	169	120	51	122	215	74	0.72
FT02	11040	20/01/2009	16/02/2009	41	41	26	15	1	13	30	11	0.43
FT02	11042	24/12/2008	01/06/2009	236	229	118	111	33	113	146	83	0.71
FT02	11044	10/01/2009	19/06/2009	267	267	139	128	92	66	238	29	0.51
FT03	11038	17/10/2009	31/12/2009	141	130	82	48	63	50	71	59	0.20
FT03	11259	19/10/2009	04/01/2010	134	125	72	53	35	50	85	40	0.17
FT03	11260	20/10/2009	09/01/2010	156	155	101	54	42	82	122	33	0.23
FT03	11262	23/10/2009	18/01/2010	169	169	114	55	45	100	144	25	0.28
FT03	11263	21/10/2009	09/01/2010	157	156	114	42	12	91	116	40	0.16
FT04	11042	08/03/2010	25/05/2010	97	51	0	51	0	0	38	13	0.24
FT04	11044	20/02/2010	19/08/2010	314	128	0	128	2	0	95	33	0.23
FT04	11261	15/02/2010	27/02/2010	13	6	0	6	1	0	4	2	0.21
FT04	11404	20/02/2010	25/09/2010	418	125	1	124	1	0	82	43	0.28
FT04	11432	12/03/2010	15/09/2010	309	112	0	112	0	0	87	25	0.33
FT06	10946	04/11/2010	19/01/2011	150	101	61	40	7	44	101	0	
FT06	11035	04/11/2010	09/01/2011	120	102	84	18	35	53	102	0	0.30
FT06	11038	02/11/2010	25/01/2011	162	88	66	22	70	48	88	0	
FT06	11262	22/10/2010	30/12/2010	136	6	3	3	0	2	6	0	0.24
FT06	11263	09/09/2010	24/11/2010	140	59	26	33	1	26	59	0	0.16
Total				4498	3388	1776	1612	524	1244	2621	767	

ESSDD
5, 853–891, 2012

Table 2. Correction coefficient calculated for each flouoremeter tag (see methods for details).

Deployment number	CTD-Fluo SRDL number	αj			βj			$\delta \cdot \alpha j$			$\delta \cdot \alpha j \cdot \beta j$		
		Mean	Lower	Upper	Mean	Lower	Upper	Mean	Lower	Upper	Mean	Lower	Upper
FT01	10863	0.26	0.13	0.46	2.96	2.20	3.77	**0.65**	0.32	1.16	1.91	0.92	3.52
FT02	10946	0.24	0.12	0.45	4.74	4.44	5.04	**0.61**	0.30	1.14	2.90	1.41	5.38
FT02	11034	0.33	0.18	0.50	2.08	1.65	2.51	**0.83**	0.47	1.26	1.73	0.93	2.72
FT02	11035	0.29	0.17	0.42	1.90	1.74	2.06	**0.74**	0.44	1.08	1.39	0.83	2.08
FT02	11039	0.14	0.09	0.20	8.74	7.77	9.75	**0.36**	0.22	0.51	3.12	1.88	4.49
FT02	11040	0.24	0.14	0.35	3.49	2.90	4.07	**0.61**	0.36	0.89	2.11	1.22	3.20
FT02	11042	0.19	0.12	0.27	3.50	3.32	3.67	**0.48**	0.30	0.68	1.67	1.05	2.36
FT02	11044	0.22	0.14	0.32	1.81	1.44	2.21	**0.57**	0.35	0.81	1.02	0.59	1.50
FT03	11038	0.11	0.10	0.12	3.58	2.74	4.46	**0.28**	0.25	0.31	1.00	0.75	1.28
FT03	11259	0.23	0.21	0.26	2.42	1.77	3.10	**0.59**	0.52	0.66	1.42	1.02	1.86
FT03	11260	0.22	0.19	0.24	2.07	1.69	2.44	**0.54**	0.48	0.61	1.13	0.89	1.36
FT03	11262	0.22	0.19	0.25	3.79	3.38	4.18	**0.56**	0.49	0.63	2.10	1.77	2.45
FT03	11263	0.27	0.23	0.30	2.29	1.90	2.71	**0.67**	0.59	0.76	1.54	1.23	1.89
FT04	11042	0.30	0.22	0.38	3.42	2.99	3.87	**0.76**	0.57	0.96	2.61	1.89	3.41
FT04	11044	0.35	0.26	0.45	2.61	2.24	3.01	**0.89**	0.66	1.15	2.33	1.65	3.09
FT04	11261	0.24	0.18	0.30	2.39	1.56	3.28	**0.61**	0.46	0.75	1.45	0.88	2.13
FT04	11404	0.25	0.19	0.31	5.07	4.51	5.64	**0.63**	0.48	0.80	3.21	2.37	4.14
FT04	11432	0.24	0.18	0.31	2.83	2.51	3.18	**0.62**	0.46	0.78	1.75	1.28	2.25
FT06	10946	0.24	0.12	0.45	4.06	3.68	4.45	**0.61**	0.31	1.13	2.49	1.24	4.59
FT06	11035	0.36	0.32	0.39	3.11	2.48	3.74	**0.90**	0.81	0.99	2.80	2.19	3.42
FT06	11038	0.25	0.12	0.46	4.24	2.99	5.60	**0.62**	0.30	1.16	2.63	1.20	5.23
FT06	11262	0.36	0.32	0.39	2.72	1.58	3.91	**0.90**	0.82	0.99	2.45	1.44	3.55
FT06	11263	0.21	0.19	0.23	1.95	1.44	2.45	**0.53**	0.48	0.58	1.04	0.76	1.32
Mean		0.24	0.20	0.29	3.04	2.53	3.57	0.61	0.51	0.73	1.99	1.44	2.33

ESSDD
5, 853–891, 2012

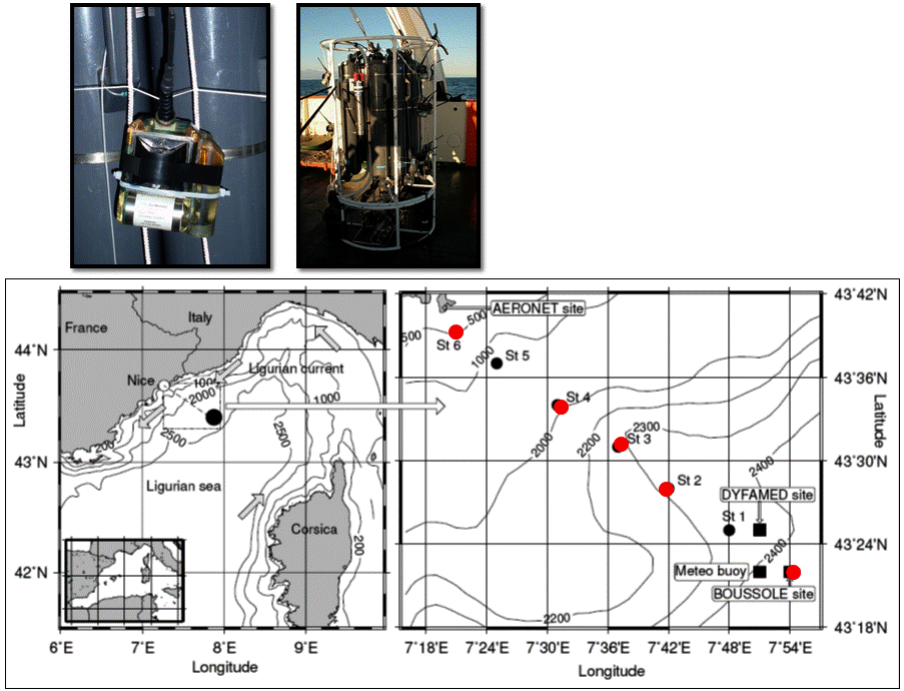

Fig. 1. Top: CTD-FLUO-SRDL were fixed on the external part of the CTD-cage. Bottom: the Boussole at sea test set up. Fluoresecence profiles were conducted on stations located on the transect between Villefranche sur mer and the BOUSSOLE site (right). A flurorescence profile combined with water sampling for HLPC assessment of Chlorophyll *a* concentration was performedat the BOUSSOLE site located 70 miles off Villefranche sur mer (left).

ESSDD
5, 853–891, 2012

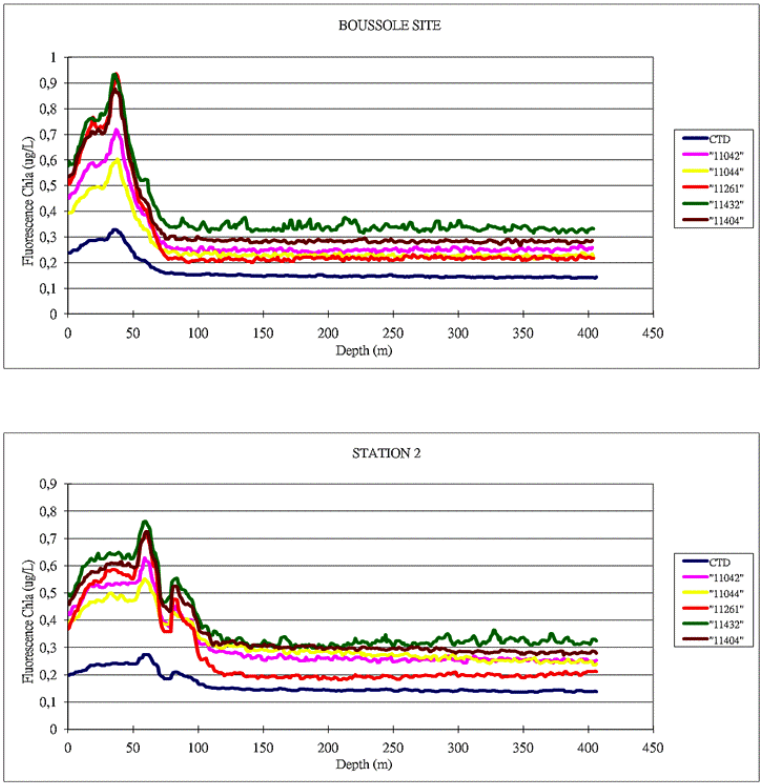

Fig. 2. Example of fluoresecence profiles provided by different CTD-FLUO-SRDLs and the reference fluorometer (in blue) obtained at two different stations. These profiles exhibit the existence of a fluorescence offset differing between CTD-FLUO-SRDLs. Fluorometers were providing consistent data between each other but differed in the absolute amount of fluorescence produced.

ESSDD
5, 853–891, 2012

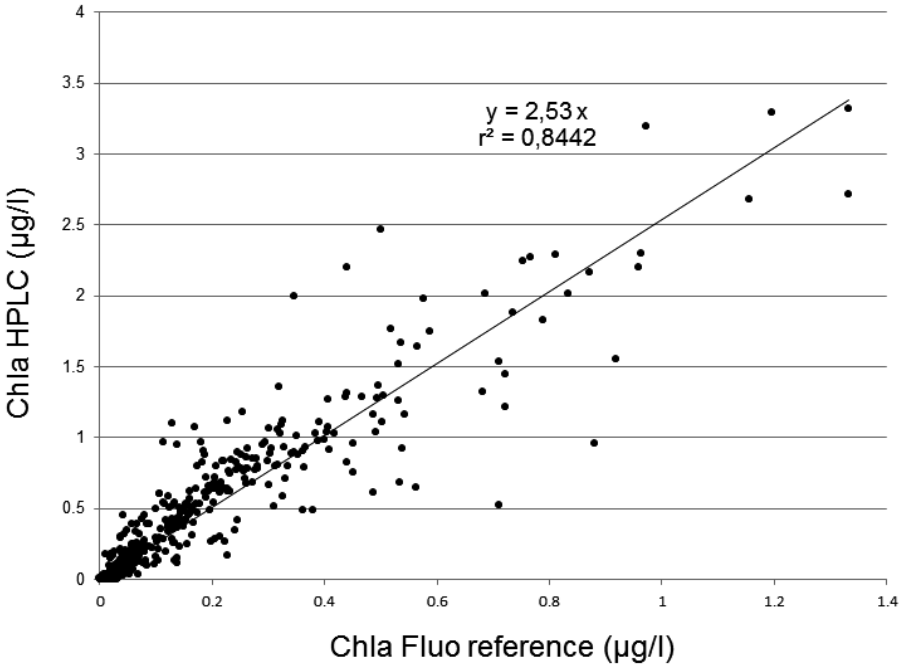

Fig. 3. Relationship between the chl *a* concentration provided by the reference fluorometer and the Chlorophyll *a* concentration estimated from HPLC measurements. This relationship was estimated over 70 test profiles ranging between 30 to 200 m and performed between 2002 and 2009.

ESSDD
5, 853–891, 2012

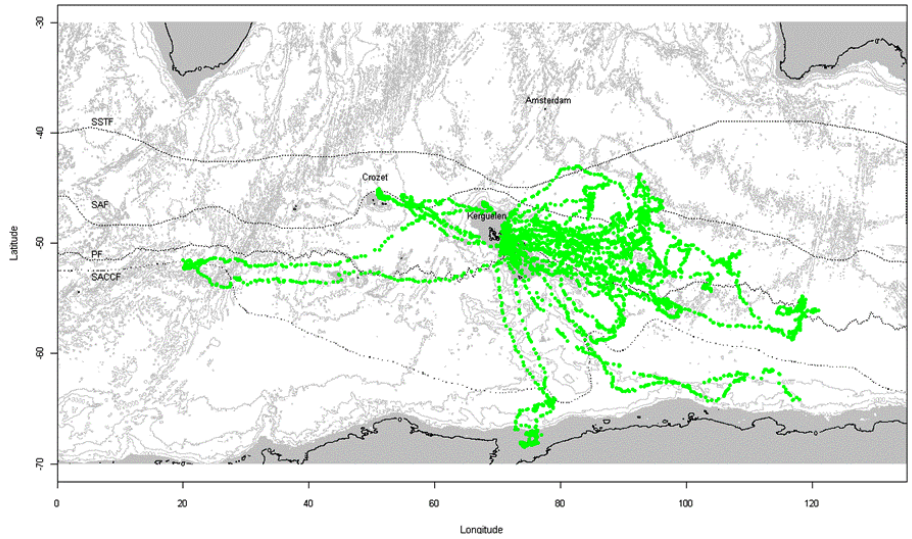

Fig. 4. Location of the fluorescence profiles along the tracks of 24 SES successfully equipped with a CTD-FLUO-SRDL and collected within the scope of this study (December 2007–January 2011).

ESSDD
5, 853–891, 2012

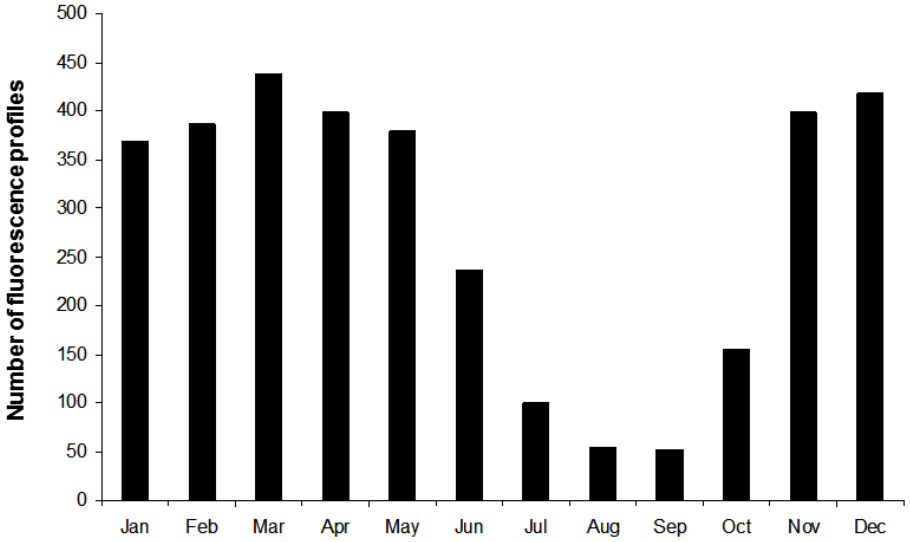

Fig. 5. Monthly distribution of the fluorescence profiles.

ESSDD
5, 853–891, 2012

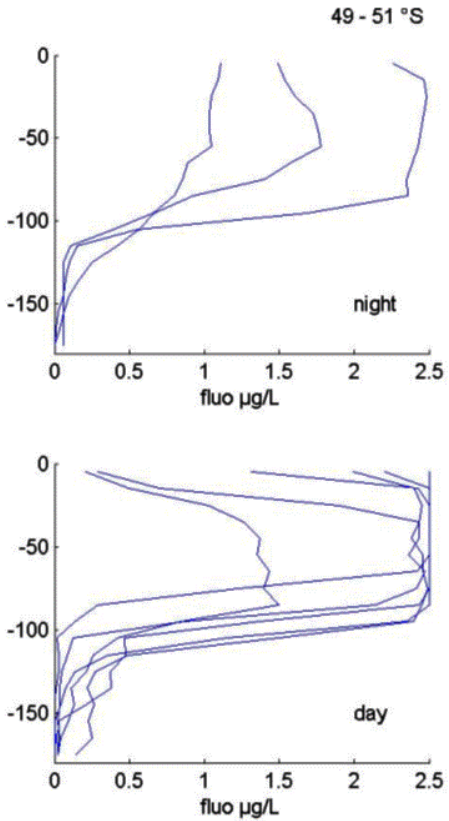

Fig. 6. Example of unquenched night fluorescence profiles (top) and quenched day ones (bottom) collected on the same location and same period by a CTD-FLUO-SRDL deployed on a male SES foraging over the Kerguelen plateau.

ESSDD
5, 853–891, 2012

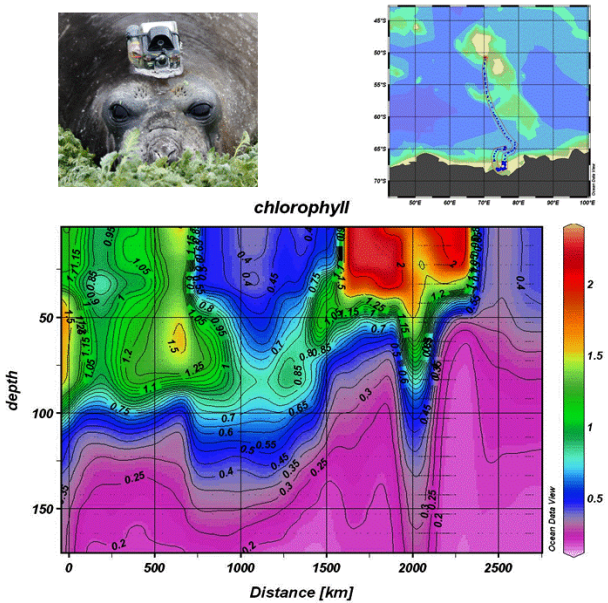

Fig. 7. Top: female SES equipped with a CTD-FLUO-SRDL and section to the track followed by a juvenile SES female between January–April 2009. This female left Kerguelen on 12 January and reached the Antarctic shelf on 6 February. This female left the Antarctic shelf on 14 March, the female then remained associated with the marginal ice zone and the Antarctic divergence. Bottom: interpolated quenching corrected fluorescence profiles provided by this SES along its track expressed as the distance (in km) covered by the seal. This tag exhibited a fluorescence offset of 0.2 $\mu g\,l^{-1}$ of chl *a* and Antarctic values higher than 2 $\mu g\,l^{-1}$ were saturated. The abrupt change in chl *a* concentration (2400 km) coincide with sea-ice formation which took place in mid march. These data show both the latitudinal change in the phytoplankton concentration along a north south transect performed during the inward trip (i.e. 1600 km south of Kerguelen 500 m isobath) and the transition in phytoplankton concentration in Antarctic waters from summer to fall (from 1600 to 2400 km).

ESSDD
5, 853–891, 2012

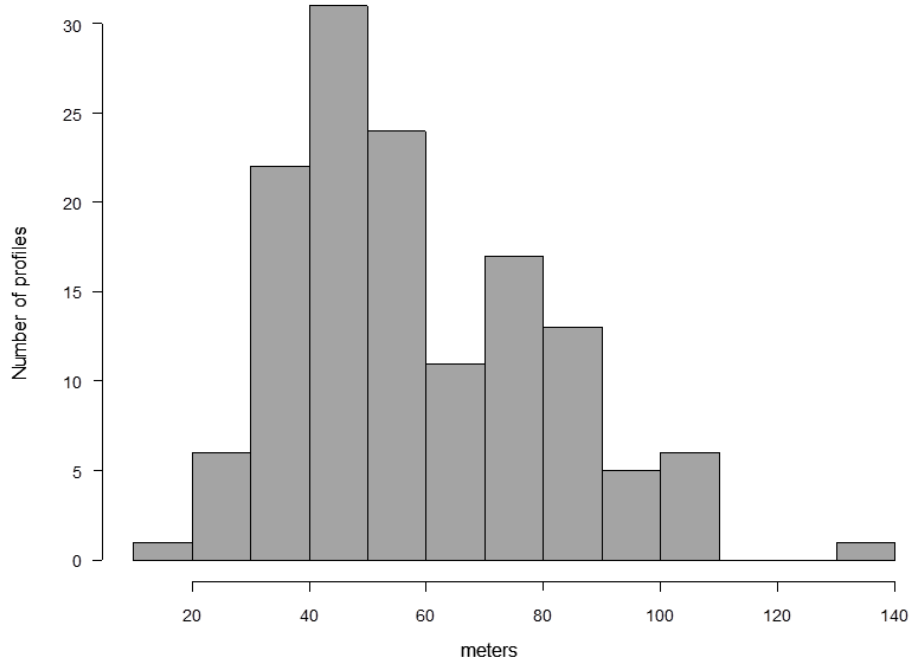

Fig. 8. Depth distribution of chl *a* maxima exceeding 30 % of the surface values pooled in 10 m depth class.

ESSDD
5, 853–891, 2012

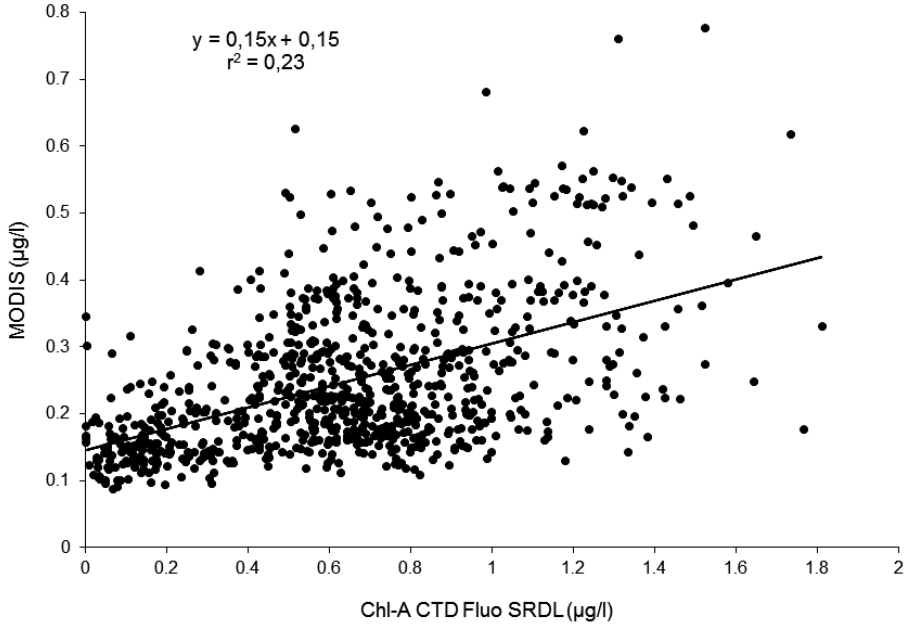

Fig. 9. Relationship between the offset, quenching corrected HPLC inter-calibrated fluorometers with the corresponding 9 km weekly MODIS data.

ESSDD
5, 853–891, 2012